



Article

Surface Charge Effects on Adsorption of Solutes by Poplar and Elm Biochars

Steven C. Peterson ^{*}, Sanghoon Kim and Jason Adkins

Plant Polymer Research, National Center for Agricultural Utilization Research, Agricultural Research Service, United States Department of Agriculture, 1815 North University Avenue, Peoria, IL 61604, USA; Sanghoon.Kim@usda.gov (S.K.); Jason.Adkins@usda.gov (J.A.)

* Correspondence: Steve.Peterson@usda.gov

Abstract: Elm and poplar are two tree species that can provide a large amount of low-value feedstock for biochar production due to their rapid growth rate (poplar), and susceptibility to disease and/or infestation (both elm and poplar). Biochar has been studied recently as filtration medium for water purification, as it provides a renewable alternative to activated carbon. In this work, the adsorption efficiency of biochars made from elm and poplar as a function of pyrolysis temperature were studied by ultraviolet (UV) adsorption of dyes with positive, neutral, and negative charges to determine what factors had the greatest effect on adsorption of these dyes. It was found that conductivity of the biochars increased with pyrolysis temperature, and that this factor was more important than surface area in terms of adsorbing charged dyes. Both elm and poplar biochars were not effective in adsorbing neutral dyes. This research demonstrates that elm and poplar biochars adsorb charged (either positively or negatively) solutes more efficiently than uncharged ones because they carry both charges themselves. Therefore, these biochars would make excellent candidates as renewable filtration media for charged contaminants.

Keywords: biochar; elm; poplar; adsorption; water filtration



Citation: Peterson, S.C.; Kim, S.; Adkins, J. Surface Charge Effects on Adsorption of Solutes by Poplar and Elm Biochars. *C* **2021**, *7*, 11. <https://doi.org/10.3390/c7010011>

Received: 9 December 2020
Accepted: 22 January 2021
Published: 26 January 2021

Publisher's Note: MDPI stays neutral with regard to jurisdictional claims in published maps and institutional affiliations.



Copyright: © 2021 by the authors. Licensee MDPI, Basel, Switzerland. This article is an open access article distributed under the terms and conditions of the Creative Commons Attribution (CC BY) license (<https://creativecommons.org/licenses/by/4.0/>).

1. Introduction

Biochar is a form of charcoal that can be made from biomass; it is defined as the solid, carbon-containing material that results from the thermochemical treatment of biomass in the absence of oxygen [1]. When biochar is made from wood, its vascular nature makes the biochar very porous [2,3]. Since wood biochar is both carbon-containing and porous, this makes it an excellent candidate for water filtration applications and this is an active area of research [4–7]. Wood is one of many different renewable biomass feedstocks for biochar, other low-cost materials being studied for filtration applications include algae [8], seaweed [9], crab shells [10], and cassava slag [11], just to name a few.

Elm and poplar are two species of trees native to the United States that are both susceptible to disease/infestation via Dutch elm disease [12] and outbreaks from tent caterpillars and gypsy moths [13], respectively. Healthy poplar trees are a rapidly growing species that flourishes in Canada and the northern United States from the Great Lakes region eastward to New England. Poplar trees can also be coppiced; this is a procedure where wood is cut from the main stump of a tree and then new shoots are regrown from the same stump and the wood is periodically re-harvested, so that a finite area of trees can continually produce lumber [14–16]. Poplar has been coppiced as a short-rotation energy crop in poorer soils and highlands [17]. As a result of both disease and the rapid growth rate of poplar, these two tree species generate massive amounts of low-value wood annually. Because of the high temperature of the pyrolysis process, any residual caterpillar/moth tissue or Dutch elm disease present are completely volatilized and do not affect the resulting biochar properties. Thus, low value elm and poplar wood make excellent feedstock for biochar in this application.

In addition to its porosity, biochar frequently has a charged surface resulting from polar functional groups. Protonation and deprotonation of these groups can occur to create a net charge on the biochar, forming an electrical double layer near the surface [18], or the polar functional groups may directly interact with analyte molecules in solution [19,20]. The purpose of this study was to observe how the surface charge of elm and poplar biochars change with pyrolysis temperature. Demonstrating the ability to manipulate the surface charge of these biochars increases their utility in adsorbing different analytes depending on the application needed. In this work three common dyes were chosen to represent positive, neutral, and negative dyes in pH 7 water. These dyes were methylene blue (net positive charge @ pH 7), fluorescein (neutral charge @ pH 7), and Coomassie blue (net negative charge @ pH 7).

2. Materials and Methods

2.1. Materials Used

Biochars made from elm and poplar at three different pyrolysis temperatures (500, 700, and 900 °C) were supplied by Biochar Options (Whitewater, WI) and used as delivered. For all biochar samples produced, yield ranged from 23–26% biochar weight/starting feedstock weight. Coomassie Brilliant Blue G-250 (CB) was purchased from Bio-Rad (Hercules, CA, USA). Methylene blue (MB) and fluorescein (F) were purchased from Sigma-Aldrich (St. Louis, MO, USA). Structural diagrams of these dyes as well as their net charge at pH 7 are shown in Figure 1.

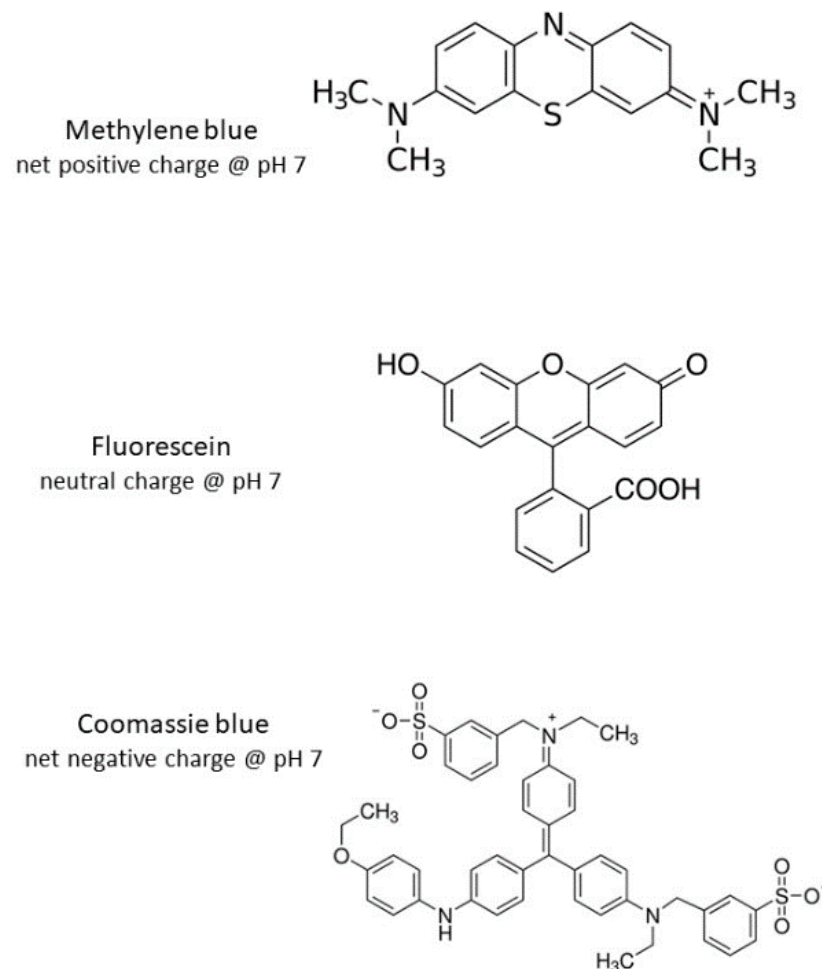


Figure 1. Structural diagrams of methylene blue (top, positively charged), fluorescein (center, neutral charge), and Coomassie blue (bottom, negatively charged) at a pH of 7.

2.2. Chemical and Physical Properties

Elemental analysis of carbon (C), hydrogen (H), and nitrogen (N) were carried out using a Perkin Elmer 2400 CHNS/O series II analyzer (Norwalk, CT, USA) using cysteine as a standard. Each measurement used approximately 2 mg of biochar and was done in triplicate. Ash content was determined using a TA Instruments Q2950 thermogravimetric analyzer (New Castle, DE, USA) by heating to 1000 °C at a heating rate of 10 °C min⁻¹ in an air atmosphere. Ash content was determined to be the weight percentage remaining, and oxygen (O) was determined by difference from the original dried sample and the sum of C, H, N, and ash. Biochar absolute density [21] and surface areas [22] were measured as detailed in previous manuscripts.

2.3. Dye Adsorption Studies

Dye solutions were prepared by dissolving 20 mg of dye in 1 L of DI water. Samples of biochar (50–500 mg biochar) were weighed into 20 mL scintillation vials, then 10 g of dye solution was added. Each sample was stirred for 1 h, then the biochar/dye suspensions were centrifuged for 10 min at 14,000 × g using an Eppendorf MiniSpin Plus microcentrifuge (Eppendorf, Hamburg, Germany). After centrifugation, the supernatant was carefully pipetted from the microcentrifuge tube, then transferred to a new scintillation vial.

Each centrifuged biochar-treated dye solution was then measured using a UV-2600 ultraviolet–visible (UV-Vis) spectrophotometer (Shimadzu Corp., Kyoto, Japan). The samples were scanned in the range of 190–800 nm using deionized (DI) water in the reference cuvette. The peak UV adsorption value was recorded and compared to the peak UV adsorption of the original dye solution to see the amount of adsorption of the dyes by the biochars. (Peak UV adsorption differed for each dye as follows: CB, 580–610 nm; MB, 660–665 nm; F, 485–490 nm). All dye adsorption experiments were conducted at room temperature.

2.4. Conductivity Measurements

Conductivity measurements were taken at room temperature using a SevenExcellence S470 pH/conductivity meter (Mettler-Toledo, Columbus, OH, USA). DI water or dye solution (100 g) was weighed into a beaker, and conductivity of the water or solution was measured while stirring. After 5 min, 100 mg of biochar was added to the stirring liquid, and the conductivity was measured after stabilization (~5 min). Once the conductivity was stable, an additional 100 mg biochar was added, and the new conductivity reading was recorded after stabilization. This was repeated until a total of 500 mg of biochar was added.

3. Results and Discussion

Table 1 shows the material properties of the elm and poplar biochars. Carbon content for these biochars is very high, ranging from 86% to nearly 97% carbon, with carbon content generally increasing with pyrolysis temperature. Most biochars will see an increase in the percent carbon content as pyrolysis temperature is increased due to increasing loss of volatile components of the feedstock [23]. Ash content for all of these biochars was relatively constant with all containing <3%, and since these biochars contain little hydrogen and nitrogen, by difference oxygen levels in the chars were reduced as pyrolysis temperature increased.

Table 1. Material properties of elm and poplar biochars.

Feedstock/ Pyrolysis T (°C)	C (%)	H (%)	N (%)	O (%) ^a	Ash (%)	Density (g/cm ³)	Surface Area (m ² /g)
Elm 500	86.4 ± 2.7	1.85 ± 0.07	0.15 ± 0.03	9.1	2.54	1.58	8.4
Elm 700	90.5 ± 0.7	1.12 ± 0.11	0.20 ± 0.01	5.6	2.56	1.66	318
Elm 900	94.9 ± 0.7	0.55 ± 0.06	0.33 ± 0.01	1.4	2.83	1.90	176
Poplar 500	89.3 ± 1.3	2.72 ± 0.21	<0.05 ^b	6.1	1.86	1.42	96
Poplar 700	89.1 ± 4.4	1.52 ± 0.18	<0.05 ^b	7.4	1.97	1.66	373
Poplar 900	96.5 ± 1.4	0.69 ± 0.09	0.07 ± 0.04	0.5	2.22	1.94	207

^a calculated by difference. ^b result was below the 0.05% detection limit.

Scanning electron microscope (SEM) images of the biochars can be seen in Figure 2. All of these samples were fairly fine powders with particle sizes ranging up to about 30 microns. As can be seen from the images, the biochar samples look similar visually, even though these samples have different surface areas. This indicates that the source of differences in surface area is due to differences in internal porosity of the biochar particles. The fact that these biochars reach a maximum surface area at 700 °C is consistent with the pyrolysis process as temperature is increased. As a biochar feedstock is subjected to pyrolysis and the temperature is raised, initially water and volatiles are driven off, which open up pores in the biochar structure and increase surface area. However, the surface areas of most biochars will typically reach a maximum from 500–800 °C [24]. At temperatures higher than this, decomposition and softening of some volatile components (depending on feedstock) form a melt that ‘clogs’ up pores in the biochar, and thus reduces the total surface area [25]. This behavior of the maximum surface area occurring between 500–800 °C is consistent with previous results in our lab [26] as well as others [27].

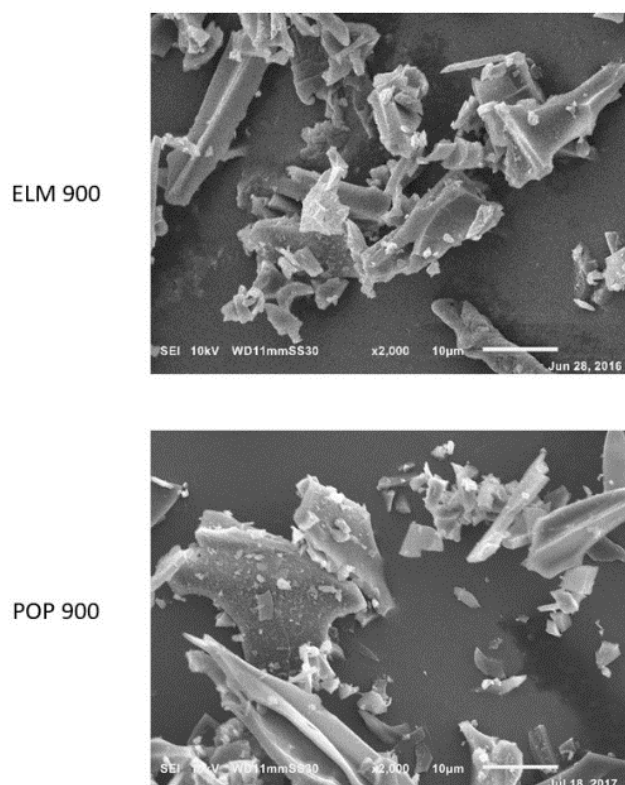


Figure 2. Scanning electron microscopy images of elm and poplar biochars at 2000×, both pyrolyzed at 900 °C. The small white bar at the lower right corner of each image represents 10 microns.

Figure 3 shows adsorption of CB dye for the poplar (A) and elm (B) biochars, respectively. These data show that the pyrolysis temperature of the biochar has a direct correlation with adsorption for the poplar biochar (Figure 3A), but appears to have no effect on the elm biochar (Figure 3B). Contrast this behavior with similar plots that show adsorption of MB dye for the poplar (Figure 4A) and elm (Figure 4B) biochars. For MB, which has a positive charge at pH 7, a trend can be seen where adsorption capability increases with pyrolysis temperature. This trend is also visible with the poplar biochar and CB, which is negatively charged in water.

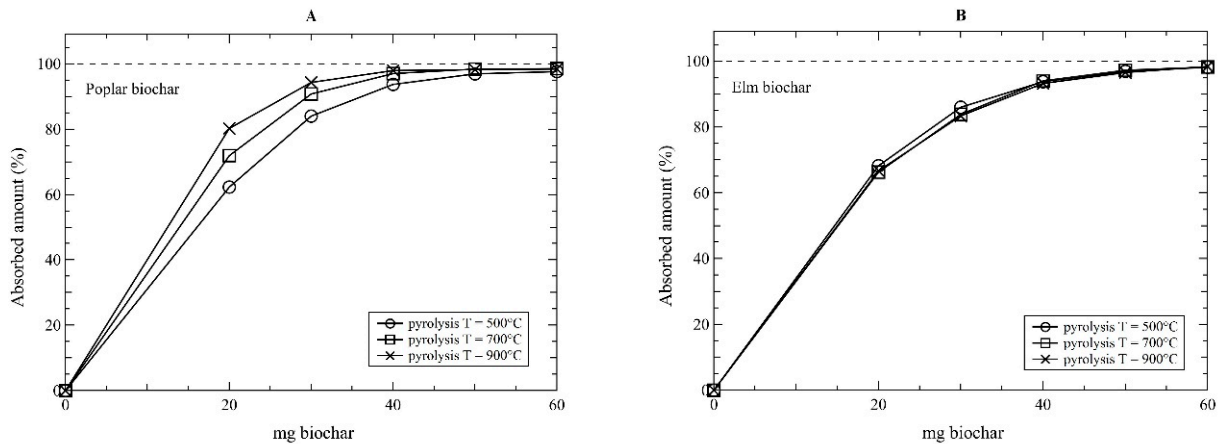


Figure 3. Adsorption of Coomassie blue as a function of added poplar (A) or elm (B) biochar for each pyrolysis temperature: 500, 700, or 900 °C.

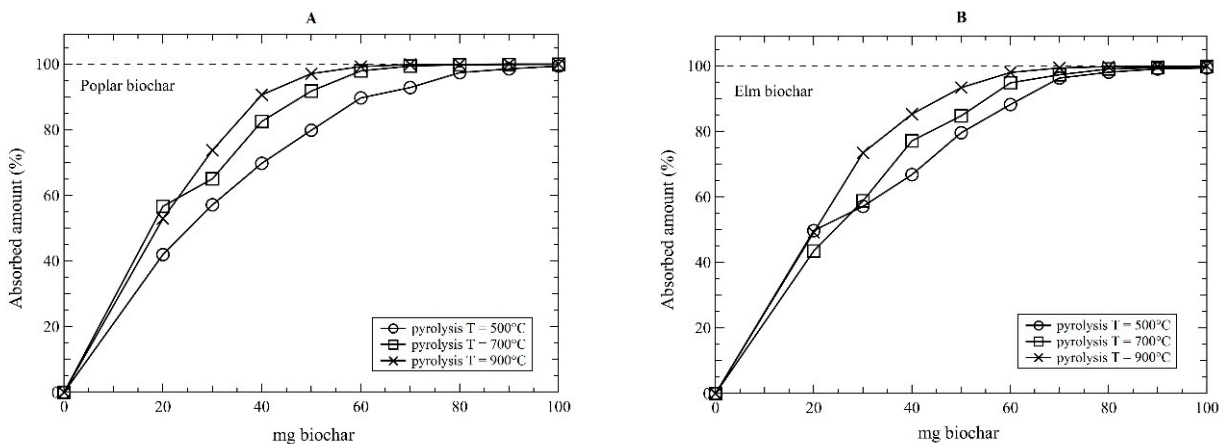


Figure 4. Adsorption of methylene blue as a function of added poplar (A) or elm (B) biochar for each pyrolysis temperature: 500, 700, or 900 °C.

One interesting aspect of these biochar samples is that they contain both positive and negative charge groups on their surface; this was evident when samples were loaded onto a microscope stage with an applied potential difference, and biochar particles could be seen migrating in both cathodic and anodic directions (see Supplementary Materials). The pyrolysis temperature of the biochars also affected the surface chemistry; Figure 5 shows the conductance per mg for each of the biochar samples, which increased directly with pyrolysis temperature. This is noteworthy because it shows that conductivity/surface charge effects apparently have a greater effect on sorption of CB and MB than surface area (see Table 1) of the biochar samples.

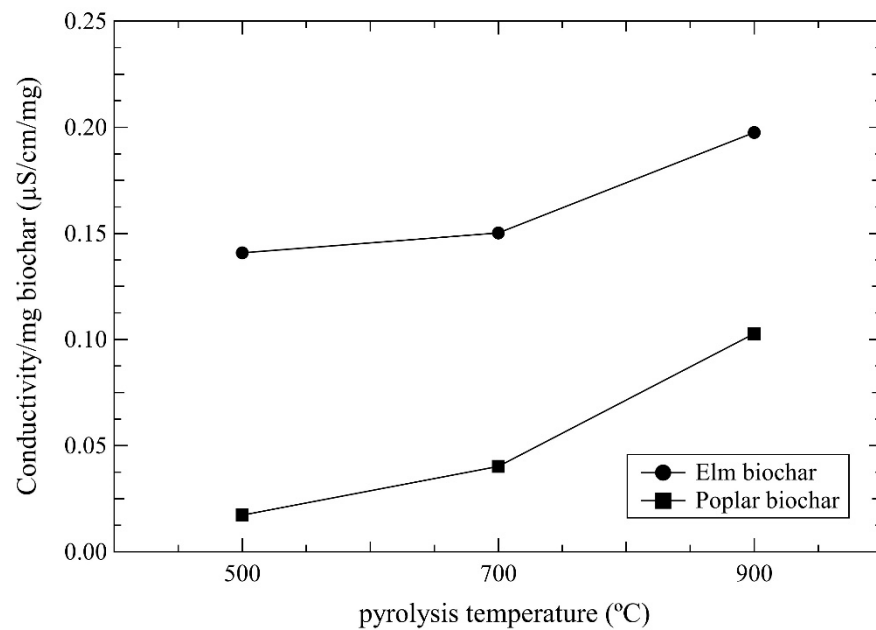


Figure 5. Conductance per mg of biochar as a function of pyrolysis temperature for both elm (circles) and poplar (squares) biochar samples.

To further test this, sorption results for the 900 °C biochar samples (highest conductivity levels) with fluorescein (F), a neutral dye at pH 7, are shown in Figure 6, along with previous results of the 900 °C biochars with methylene blue and Coomassie blue. In this figure the effects of biochar conductivity vs. surface area are clearly seen. These biochar samples are able to adsorb 100% of the charged dyes (CB and MB) at approximately 60 mg, whereas for F, the only neutral dye, 100% of the dye is not adsorbed until beyond 350 mg of biochar. Surface area of the biochars also plays a role in dye adsorption but is clearly dominated by surface charge effects. For example, comparing the two F traces in Figure 6, it can be seen that poplar biochar is a more efficient adsorbent than elm, and poplar biochar does have greater surface area than elm (207 to 176 m²/g, respectively, see Table 1).

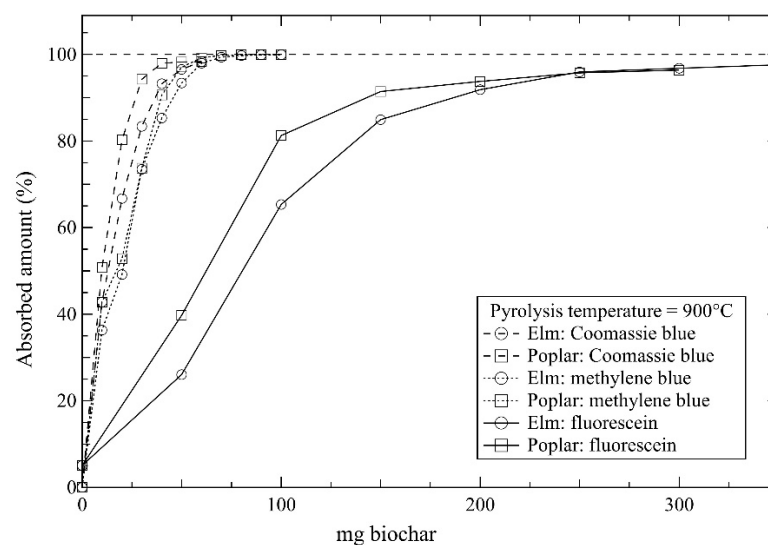


Figure 6. Adsorption of dye as a function of added elm or poplar biochars pyrolyzed at 900 °C. The dotted lines show adsorption behavior for the charged dyes Coomassie and methylene blue while the solid lines show adsorption behavior for the neutral dye fluorescein.

4. Conclusions

Poplar and elm are two species of wood that are plentiful and of low value due to rapid growth rates (poplar) and disease/infestation (both species). These wood feedstocks can be converted into biochar and used for filtration media, similar to activated carbon. Biochars from these two feedstocks are conductive in water, and this conductivity increases with pyrolysis temperature. Adsorption of the dyes Coomassie blue and methylene blue in pH 7 water (where both dyes have a net negative and positive charge, respectively) was most effective with biochars that had been pyrolyzed at the highest temperature, and therefore had the highest conductivity. The surface charge effect was more influential than the surface area of the biochars in terms of adsorbing charged dye molecules. These biochars showed poor adsorption behavior for fluorescein, a neutral dye at pH 7.

These studies indicate that by pyrolyzing poplar and/or elm at high temperature, biochars can be made that have improved adsorption capabilities for charged solutes in water. These biochars could be mixed with other sorptive media adept at adsorbing neutral contaminants to make filtration media that would be appropriate for adsorbing contaminants with any charge state.

Supplementary Materials: The following are available online at <https://www.mdpi.com/2311-5629/7/1/11/s1>, Video S1: Biochar particle migration.

Author Contributions: Conceptualization, S.C.P., S.K. and J.A.; methodology, S.C.P., S.K. and J.A.; investigation, S.K. and J.A.; writing, original draft preparation, S.C.P.; writing, review and editing, S.C.P. All authors have read and agreed to the published version of the manuscript.

Funding: This research received no external funding.

Institutional Review Board Statement: Not applicable.

Informed Consent Statement: Not applicable.

Data Availability Statement: Not applicable.

Acknowledgments: The authors would like to thank A.J. Thomas for performing CHNO analysis as well as density measurements, and Mike Jackson for providing surface area data.

Conflicts of Interest: The authors declare no conflict of interest.

References

1. Lehmann, J.; Joseph, S. *Biochar for Environmental Management: Science and Technology*, 2nd ed.; Routledge: New York, NY, USA, 2015; 976p.
2. Lee, Y.; Eum, P.-R.-B.; Ryu, C.; Park, Y.-K.; Jung, J.-H.; Hyun, S. Characteristics of biochar produced from slow pyrolysis of geodae-uksae 1. *Bioresour. Technol.* **2013**, *130*, 345–350. [[CrossRef](#)] [[PubMed](#)]
3. Liatsou, I.; Pashalidis, I.; Oezaslan, M.; Dosche, C. Surface characterization of oxidized biochar fibers derived from luffa cylindrical and lanthanide binding. *J. Environ. Chem. Eng.* **2017**, *5*, 4069–4074. [[CrossRef](#)]
4. Mohan, D.; Sarswat, A.; Ok, Y.S.; Pittman, C.U. Organic and inorganic contaminants removal from water with biochar, a renewable, low cost and sustainable adsorbent—A critical review. *Bioresour. Technol.* **2014**, *160*, 191–202. [[CrossRef](#)] [[PubMed](#)]
5. Inyang, M.; Dickenson, E. The potential role of biochar in the removal of organic and microbial contaminants from potable and reuse water: A review. *Chemosphere* **2015**, *134*, 232–240. [[CrossRef](#)]
6. Inyang, M.I.; Gao, B.; Yao, Y.; Xue, Y.; Zimmerman, A.; Mosa, A.; Pullammanappallil, P.; Ok, Y.S.; Cao, X. A review of biochar as a low-cost adsorbent for aqueous heavy metal removal. *Crit. Rev. Environ. Sci. Technol.* **2016**, *46*, 406–433. [[CrossRef](#)]
7. Wathukarage, A.; Herath, I.; Iqbal, M.C.M.; Vithanage, M. Mechanistic understanding of crystal violet dye sorption by woody biochar: Implications for wastewater treatment. *Environ. Geochem. Health* **2019**, *41*, 1647–1661. [[CrossRef](#)]
8. Zhou, Y.; Zhang, H.; Cai, L.; Guo, J.; Wang, Y.; Ji, L.; Song, W. Preparation and characterization of macroalgae biochar nanomaterials with highly efficient adsorption and photodegradation ability. *Materials* **2018**, *11*, 1709. [[CrossRef](#)]
9. Ahmed, M.J.; Okoye, P.U.; Hummadi, E.H.; Hameed, B.H. High-performance porous biochar from the pyrolysis of natural and renewable seaweed (*gelidiella acerosa*) and its application for the adsorption of methylene blue. *Bioresour. Technol.* **2019**, *278*, 159–164. [[CrossRef](#)]
10. Dai, L.; Zhu, W.; He, L.; Tan, F.; Zhu, N.; Zhou, Q.; He, M.; Hu, G. Calcium-rich biochar from crab shell: An unexpected super adsorbent for dye removal. *Bioresour. Technol.* **2018**, *267*, 510–516. [[CrossRef](#)]
11. Wu, J.; Yang, J.; Huang, G.; Xu, C.; Lin, B. Hydrothermal carbonization synthesis of cassava slag biochar with excellent adsorption performance for rhodamine b. *J. Clean. Prod.* **2020**, *251*, 119717. [[CrossRef](#)]

12. Santini, A.; Faccoli, M. Dutch elm disease and elm bark beetles: A century of association. *iForest-Biogeosci. For.* **2014**, *8*, 126–134. [[CrossRef](#)]
13. Lindroth, R.L.; Donaldson, J.R.; Stevens, M.T.; Gusse, A.C. Browse quality in quaking aspen (*populus tremuloides*): Effects of genotype, nutrients, defoliation, and coppicing. *J. Chem. Ecol.* **2007**, *33*, 1049–1064. [[CrossRef](#)] [[PubMed](#)]
14. Afas, N.A.; Marron, N.; Van Dongen, S.; Laureysens, I.; Ceulemans, R. Dynamics of biomass production in a poplar coppice culture over three rotations (11 years). *Forest Ecol. Manag.* **2008**, *255*, 1883–1891. [[CrossRef](#)]
15. Dillen, S.Y.; Djomo, S.N.; Al Afas, N.; Vanbeverem, S.; Ceulemans, R. Biomass yield and energy balance of a short-rotation poplar coppice with multiple clones on degraded land during 16 years. *Biomass Bioenergy* **2013**, *56*, 157–165. [[CrossRef](#)]
16. Nassi, O.; Di Nasso, N.; Guidi, W.; Ragaglini, G.; Tozzini, C.; Bonari, E. Biomass production and energy balance of a 12-year-old short-rotation coppice poplar stand under different cutting cycles. *GCB Bioenergy* **2010**, *2*, 89–97. [[CrossRef](#)]
17. Kauter, D.; Lewandowski, I.; Claupein, W. Quantity and quality of harvestable biomass from populus short rotation coppice for solid fuel use—a review of the physiological basis and management influences. *Biomass Bioenergy* **2003**, *24*, 411–427. [[CrossRef](#)]
18. Qiu, Y.; Zheng, Z.; Zhou, Z.; Sheng, G.D. Effectiveness and mechanisms of dye adsorption on a straw-based biochar. *Bioresour. Technol.* **2009**, *100*, 5348–5351. [[CrossRef](#)]
19. Chen, B.; Zhou, D.; Zhu, L. Transitional adsorption and partition of nonpolar and polar aromatic contaminants by biochars of pine needles with different pyrolytic temperatures. *Environ. Sci. Technol.* **2008**, *42*, 5137–5143. [[CrossRef](#)]
20. Yang, Y.; Chun, Y.; Sheng, G.; Huang, M. Ph-dependence of pesticide adsorption by wheat-residue-derived black carbon. *Langmuir* **2004**, *20*, 6736–6741. [[CrossRef](#)]
21. Peterson, S.C.; Chandrasekaran, S.R.; Sharma, B.K. Birchwood biochar as partial carbon black replacement in styrene–butadiene rubber composites. *J. Elastomers Plast.* **2015**, *48*, 305–316. [[CrossRef](#)]
22. Vaughn, S.F.; Kenar, J.A.; Tisserat, B.; Jackson, M.A.; Joshee, N.; Vaidya, B.N.; Peterson, S.C. Chemical and physical properties of paulownia elongata biochar modified with oxidants for horticultural applications. *Ind. Crops Prod.* **2017**, *97*, 260–267. [[CrossRef](#)]
23. Uchimiya, M.; Wartelle, L.H.; Klasson, K.T.; Fortier, C.A.; Lima, I.M. Influence of pyrolysis temperature on biochar property and function as a heavy metal sorbent in soil. *J. Agric. Food Chem.* **2011**, *59*, 2501–2510. [[CrossRef](#)] [[PubMed](#)]
24. Downie, A. Biochar Production and Use: Environmental Risks and Rewards. Ph.D. Thesis, University of New South Wales, Sydney, Australia, 2011.
25. Lua, A.C.; Yang, T.; Guo, J. Effects of pyrolysis conditions on the properties of activated carbons prepared from pistachio-nut shells. *J. Anal. Appl. Pyrol.* **2004**, *72*, 279–287. [[CrossRef](#)]
26. Peterson, S.C.; Jackson, M.A. Simplifying pyrolysis: Using gasification to produce corn stover and wheat straw biochar for sorptive and horticultural media. *Ind. Crop. Prod.* **2014**, *53*, 228–235. [[CrossRef](#)]
27. Brown, R.A.; Kercher, A.K.; Nguyen, T.H.; Nagle, D.C.; Ball, W.P. Production and characterization of synthetic wood chars for use as surrogates for natural sorbents. *Org. Geochem.* **2006**, *37*, 321–333. [[CrossRef](#)]